SILICON ISOTOPES IN GRANULITE XENOLITHS: INSIGHTS INTO ISOTOPIC FRACTIONATION DURING IGNEOUS PROCESSES AND THE COMPOSITION OF THE DEEP CONTINENTAL CRUST

Paul S. Savage[1#]*, R. Bastian Georg[2], Helen M. Williams[3] & Alex N. Halliday[1]

[1]Department of Earth Sciences, University of Oxford, South Parks Road, Oxford, OX1 3AN, UK

[#]now at: Department of Earth and Planetary Sciences, Washington University in St. Louis, One Brookings Drive, St. Louis, MO, USA. Tel: +1-(314)-935-5619 / Fax: +1-(314)-935-7361

[2]Water Quality Centre, Trent University, 1600 West Bank Drive, Peterborough, Ontario, K9J 7B8, Canada

[3]Department of Earth Sciences, Durham University, Science Labs, Durham DH1 3LE, UK

*corresponding author: savage@levee.wustl.edu

ABSTRACT

The silicon (Si) cycle is of great current interest but the isotopic composition of the continental crust has not been determined. Magmatic differentiation generates liquids with heavier Si and the lower crust, thought to be dominated by cumulates and restites, is predicted to have a light isotopic composition. This is borne out by the composition of many types of granite, which appear to have relative light Si for their silica content. Here we report the Si isotopic compositions of two granulite facies xenolith suites, from the Chudleigh and McBride volcanic provinces, Australia, providing new constraints on deep crustal processes and the average composition of the deep continental crust.

The xenoliths display a range of isotopic compositions (δ^{30}Si = -0.43 to -0.15 ‰) comparable to that measured previously for igneous rocks. The isotopic compositions of the McBride xenoliths reflect assimilation and fractional crystallisation (AFC), or partial melting processes. Silicon and O isotopes are correlated in the McBride suite and can be explained by AFC of various evolved parent melts. In contrast, the Chudleigh xenoliths have Si isotope compositions predominantly controlled by the specific mineralogy of individual cumulates. Using the xenolith data and a number of weighting methods, the Si isotope composition of the lower and middle crust are calculated to be δ^{30}Si = -0.29 ± 0.04 ‰ (95% s.e.) and -0.23 ± 0.04 ‰ (95% s.e.) respectively. These values are almost identical to the composition of the Bulk Silicate Earth, implying minimal isotope fractionation associated with continent formation and no light lower crustal reservoir.

Keywords: Silicon isotopes; lower continental crust; granulite xenoliths; igneous processes; AFC

1. INTRODUCTION

Silicon (Si) is the 2nd-most abundant element in the Earth's continental crust (Si ~28 wt.%; Rudnick and Gao, 2003) and is an important element in many geo- and biochemical cycles (e.g. Tréguer et al., 1995, Basile-Doelsch, 2006). This "Si biosphere" is fed by chemical weathering, which forms secondary minerals associated with large negative Si isotope fractionation (Ziegler et al., 2005a&b; Opfergelt et al., 2012) and a complementary heavy Si fluid phase (De la Rocha et al., 2000; Georg et al., 2009a). The exact Si isotopic composition of the protolith itself, that is the continental crust, is not well constrained but this can now be achieved with multi collector inductively-coupled-plasma mass-spectrometry (MC-ICP-MS). These instruments have made it possible to precisely and accurately analyse all three stable isotopes (^{28}Si, ^{29}Si and ^{30}Si) at high mass resolution (e.g. Georg et al., 2006). Small isotopic variations generated through igneous processes are now detectable, and this in turn, has permitted valuable and novel insights into how Si isotopes behave in high temperature environments.

It is now known that the mantle is effectively homogeneous with respect to Si isotopes. The resultant composition of the Bulk Silicate Earth (BSE) is well–defined (Savage et al., 2010) with a value of $\delta^{30}Si$ = -0.29 ± 0.08‰ (2 s.d.), where $\delta^{30}Si=[(^{30}Si/^{28}Si_{sample})/(^{30}Si/^{28}Si_{standard})-1]\times1000$. Magmatic differentiation of basalt results in enrichment of the heavier isotopes in the evolved products (Fig. 1), with rhyolites having $\delta^{30}Si$ of ~ -0.15 ‰ (Savage et al., 2011). This isotope fractionation appears predictable and linked to SiO_2 as follows:

$$\delta^{30}Si\ (‰) = 0.0056 \times SiO_2\ (wt.\%) - 0.567\ (\pm 0.05;\ 2\ s.e.\ of\ the\ regression);$$

termed the "igneous array" for Si isotopes. Deviations from this array can be used as evidence of sediment anatexis and assimilation, which is consistent with the composition of many granites (Zambardi and Poitrasson, 2011; Savage et al., 2012). Surprisingly, this is not just true of S-type granites; I-types also display a broad range of isotopic compositions for their silica content unlike the products of differentiation or melting of juvenile basaltic crust. Therefore, the deep crust from which silicic magmas are largely derived appears to be highly heterogeneous with respect to Si isotopes, consistent with it being the site of protracted geological processes that have introduced material from both surface and mantle reservoirs.

This paper tests this with the first high precision Si isotope data for samples of the deep crust itself. This study also assesses (a) how cumulate formation and melt depletion affect Si isotope composition, and (b) the average Si isotope composition of the deep continental crust. If anything the average deep crust might be expected to be isotopically light. This is because Si isotope fractionation relates to degree of polymerisation (Grant, 1954), wherein the least refractory, more Si-rich and, hence, isotopically heavier phases are expected to be the first to melt, even though the presence of various “network-modifying” cations such as Al can affect this relationship (e.g. Méheut et al., 2009). The Si isotope composition of less Si-rich phases (clinopyroxene and olivine) is indeed isotopically lighter than coexisting plagioclase (in samples from the Skaergaard Complex, Greenland; Fig. 1, Savage et al., 2011). Deep continental crust includes, cumulate and restitic material as significant components (Kempton and Harmon, 1992), which should bias the bulk composition towards isotopically lighter compositions.

2. SAMPLES FROM THE DEEP CONTINENTAL CRUST

The continental crust can be split into three layers, upper, middle and lower, defined on the basis of seismological profiles (e.g. Holbrook et al., 1992; Rudnick and Fountain, 1995) and examination of exhumed crustal sequences (e.g. Fountain and Salisbury, 1981;

Bohlen and Mezger, 1989). In general, these layers also correspond to changes in metamorphic facies, depending on temperature gradient. For an average crustal thickness of ~40 km, the upper continental crust (UCC) comprises the top 25 – 35% of the total crustal thickness (10-15km depth); this reservoir is composed predominantly of felsic granitoid material with significant sedimentary and metamorphic components. Below the UCC is the middle continental crust (MCC), comprising around 30 % of the total crustal thickness (between 10-15 km and 20-25 km depth) The MCC is composed of amphibolite and lower-granulite facies, predominantly andesitic meta-igneous and meta-sedimentary rocks. The lowest ~35% of the crust (below 20-25 km depth) the lower continental crust (LCC) is more primitive, consisting predominantly of granulite facies mafic meta-igneous rocks, with a minor but significant proportion of meta-sedimentary material (see Rudnick and Gao, 2003, and references therein). In the following, the MCC and LCC together will be described as the "deep continental crust".

Representative samples of the upper continental crust are readily available, such that the Si isotopic compositions of lithologies from this reservoir are comparatively well-studied (cf. Douthitt, 1982; Ding et al., 1996; Savage et al., 2012a&b). Samples of the MCC and LCC are more scarce than for the UCC, but they are available. In the main, two sample types have been utilised to investigate the composition of the deep crust. These are tectonically-exhumed high-grade metamorphic terranes (e.g. Bohlen and Mezger, 1989) and granulite facies xenoliths erupted through volcanic conduits (e.g. Dawson, 1977; Rudnick et al., 1986; Rudnick and Taylor, 1987; Condie and Selverstone, 1999; Villaseca et al., 1999; Liu et al., 2001). Many granulite facies xenoliths are of higher metamorphic grade and are thought to be derived from the LCC, whereas terranes, typically of amphibolite and lower granulite facies, are most likely representative of the MCC (Bohlen and Mezger, 1989).

In this study, we have chosen to analyse xenolith material as opposed to granulite terrane samples, specifically a set of 16 granulite facies xenoliths, taken from the McBride and Chudleigh volcanic provinces, Queensland, Australia. This is because xenoliths are erupted relatively instantaneously from the deep crust, whereas terranes are typically exhumed over millions of years. This reduces the effect of retrograde metamorphism to negligible levels; only garnets appear to have undergone decompression reactions in the xenoliths which we have analysed (Rudnick et al., 1986; Rudnick and Taylor, 1987). It also limits the scope for any metasomatic processes that could affect Si elemental and isotopic composition.

The question as to how representative granulite facies xenoliths of the LCC is important to consider, as use of such material may bias estimates of the bulk Si isotopic composition of the deep crust. Specifically, felsic xenoliths may not survive transport in a magma hotter than their solidus. However, Rudnick and Fountain (1995) conclude that this should only happen if the crust was already partially molten before eruption. Even so, given the risk of bias, we have taken this into account in our calculations of crustal composition (Section 5.4).

2.1 McBride xenolith suite, Queensland, Australia

Eight granulite xenolith samples from the McBride volcanic province, northern Queensland, were analysed for Si isotopes. These samples were taken from a suite already well-characterised for major and trace elements, as well as radiogenic (Sr, Nd, U, Pb, Os) and stable (Li, O) isotopes (Rudnick and Taylor, 1987; Rudnick and Williams, 1987; Rudnick, 1990; Kempton and Harmon, 1992; Saal et al., 1998; Teng et al., 2008).

The McBride xenoliths used in this study were first described by Rudnick and Taylor (1987). The xenoliths are hosted in a single basaltic cinder cone of late Cenozoic age, are small (< 11 cm in diameter) and display a wide range of chemical and mineralogical contents, with SiO_2 ranging from 41 to 67 wt.%. Thermobarometric techniques indicate that most of the xenoliths equilibrated in the lower continental crust (between 26 and 40 km), with only one sample, 85-107, displaying cooler temperatures indicative of a shallower (~18 km) origin. Equilibrium mineral assemblages suggest that minimal temperature and/or pressure variations have affected the samples since peak granulite metamorphism, and post-eruptive alteration is also limited. Strontium-neodymium isotope systematics suggests that the samples formed by mixing of a mantle-derived basaltic melt with pre-existing crustal material (possibly represented by the meta-sedimentary xenoliths) and subsequent magmatic differentiation (Rudnick, 1990).

The McBride xenoliths represent a range of protoliths, providing clear evidence for a chemically heterogeneous lower crust. Of the five mafic granulite facies xenoliths analysed in this study, two are “two pyroxene granulites”, representative of basaltic melts (85-100 and 85-120). The other three are garnet-clinopyroxene granulites, two of which are melt-depleted restites (83-159 and 85-114), the other a mafic cumulate (85-107). As well as mafic material, two felsic granulites (83-160 and 83-162) composed of quartz, garnet and K-feldspar (83-160 also has major plagioclase and orthopyroxene) were analysed. These have protoliths similar to the Phanerozoic calc-alkaline granitoid rocks present at the surface in the McBride volcanic province. Intermediate-composition granulite facies xenoliths from this suite are interpreted to have a sedimentary protolith; sample 83-157 is a metapelite composed of major plagioclase, garnet quartz and orthopyroxene. All sample and protolith information is taken from Rudnick and Taylor (1987).

2.2 Chudleigh xenolith suite, Queensland, Australia

To complement the McBride suite, eight granulite facies xenoliths were analysed from the Chudleigh volcanic province, northern Queensland, Australia. As with the above samples, the Chudleigh xenoliths were taken from a suite already well-characterised for major and trace elements as well as radiogenic (Sr, Nd, Pb, Os) and stable (O, Li) isotopes (Rudnick et al., 1986; Rudnick and Goldstein., 1990; Kempton and Harmon., 1992; Saal et al., 1998; Teng et al., 2008).

The Chudleigh xenoliths used in this study are described in detail by Rudnick et al. (1986). They are hosted in Plio-pleistocene alkali basaltic vents, are large (between 5 and 50 cm), blocky and coarse-grained. Unlike the McBride xenoliths, these samples show little variation in silica contents, ranging from 49 to 51 wt.%. All the samples are derived from mafic igneous protoliths and display limited post-eruptive alteration.

Three types of xenolith are recognised in the Chudleigh suite (of which we have analysed a representative selection): plagioclase-rich granulites (samples 83-107, 83-112, 83-125, 83-127 and 83-131); pyroxene-rich granulites (samples 83-110 and 83-115) and transitional granulites (which show chemical and mineralogical properties that lie between the other two types; sample BC). Despite little variation in major element compositions, the large mineralogical differences indicate a wide range of equilibration depths, between 20 and 40 km, and also large temperature differences of between 600 and 1000ºC (Rudnick and Taylor, 1991). High Si/Na ratios in the samples provide evidence that the xenoliths are unlikely to represent equilibrium melt compositions, instead, they are inferred to be igneous cumulates, formed in a system where plagioclase was subordinate to ferromagnesian phases. Sr-Nd systematics suggest that the cumulates and a coexisting melt phase (which is not represented in the Chudleigh xenoliths) evolved through AFC processes (Assimilation and Fractional Crystallisation; DePaolo, 1981), whereby mantle-derived basaltic melt assimilated a pre-existing felsic crustal source and evolved through magmatic differentiation (Rudnick et al., 1986).

These two sample suites will provide important insights into the behaviour of Si isotopes in magmatic processes. First, the McBride suite, which is predominantly comprised of samples that represent equilibrium melt assemblages, can be used to confirm the robustness of the "igneous array" (Section 1), as these samples are not thought to be cogenetic. Second, the cumulate and restite samples from both the McBride and Chudleigh suites can help answer the important question as to whether these lithologies are consistently isotopically light (with respect to δ^{30}Si), which will allows us to assess whether the deep continental crust is a thus far hidden isotopically light reservoir for silicon.

3. METHODS

Xenolith samples were provided in powder form by R. Rudnick. Although the samples were powdered in agate, this method has been shown to have no significant effect on the measured Si isotope composition of a sample (Savage et al., 2011, Zambardi and Poitrasson, 2011b). This should be true even for the smaller McBride xenoliths, as these are still large (~300g) compared to the amount of agate typically added to samples during milling (~0.10 % ≈ 0.3g; Allen, 1998). All samples and standards were processed for MC-ICP-MS analysis following the HF-free alkali fusion technique as detailed by Georg et al. (2006); such techniques have been utilised successfully by many research groups for Si isotope analysis and are comprehensively described elsewhere (e.g. Fitoussi et al., 2009; Zambardi and Poitrasson, 2011b; Savage et al., 2011, 2012a).

In brief: ~10 mg of sample powder was added to a silver crucible with ~200 mg of analytical grade NaOH flux (Merck) in pellet form. The crucible was heated to 720ºC for 12 minutes, removed and left to cool, then placed in ~20 ml of MQ-e (18.2 MΩ) water. After 24 hours, the fusion cake was transferred into solution, again in MQ-e water, and acidified to 1% v/v with HNO_3. Silicon concentrations were analysed using a spectrophotometer and fusion yields were assessed. The average yield for this study was 100 ± 3 % (2 s.d.) for 16 fusions; no aliquot with a yield less than 97% was measured.

Sample solutions were purified before mass spectrometry using a single-pass column technique using BioRAD AG50W X12 200-400 mesh cation resin, and acidified to 1% v/v HNO_3 before analysis (Georg et al., 2006). There is no evidence for matrix effects from other anionic species on the measured Si isotopic ratios (Georg et al., 2006), and the external standards BHVO-2 and Diatomite were routinely analysed to assess method accuracy and reproducibility.

Isotopic measurements were made using a Nu Instruments Nu Plasma HR High Resolution Multi-Collector Inductively-Coupled-Plasma Mass Spectrometer (HR-MC-ICP-MS). Samples were aspirated using a 6 mm PFA concentric microflow nebuliser and desolvated using an Aridus II (Cetac, NE, USA). Isotopic analyses were made at "medium" resolution (resolving power $M/\Delta M \sim 3300$, where ΔM is defined at 5% and 95% for peak height; Weyer and Schwieters, 2003) to avoid poly-atomic interferences, which results in a ~ 85% reduction of instrument sensitivity. At sample Si concentrations of 750 ppb, a total signal of 1×10^{-10}A was typical.

Isotopic analyses were calculated via the standard-sample bracketing protocol, using NBS28 (NIST RM8546 silica sand) as the bracketing standard. Variations in Si isotopes are represented by the delta notation as $\delta^{30}Si$ or $\delta^{29}Si$, defined as the deviation in per mil (‰) of a sample's ratio of $^{x}Si/^{28}Si$ from the standard (NBS28), as such:

$$\delta^{30}Si = [(^{30}Si/^{28}Si_{sample})/(^{30}Si/^{28}Si_{standard}) - 1] \times 1000;$$

$$\delta^{29}Si = [(^{29}Si/^{28}Si_{sample})/(^{29}Si/^{28}Si_{standard}) - 1] \times 1000.$$

We discuss our Si isotopic data using $\delta^{30}Si$ values, which are roughly twice the magnitude of $\delta^{29}Si$ values. Assuming mass dependence, which is valid for terrestrial samples, this relationship was used as a further test for data quality.

4. RESULTS

4.1 External Standards

Sample data accuracy and precision were assessed using routine and repeated analysis of the external standards Diatomite and BHVO-2 during data acquisition. Diatomite is a natural pure silica standard (Reynolds et al., 2007; Georg et al., 2009b; Ziegler et al., 2010; Chakrabarti and Jacobsen, 2010; Armytage et al., 2011; Hughes et al., 2011; Savage et al., 2011, 2012a) and BHVO-2 is a USGS natural basaltic rock standard (Abraham et al., 2008; van den Boorn et al., 2009; Zambardi and Poitrasson, 2011b; Armytage et al., 2011; Savage et al., 2011, 2012a) that are both now widely utilised and well established in Si isotope studies. The Si isotopic data for 4 repeat runs of each standard (each on a different day) as well as the long term average, are given in Table 1. Our data for Diatomite (δ^{30}Si = 1.24 ± 0.07 ‰; 2 s.d., n = 4) and BHVO-2 (δ^{30}Si = -0.29 ± 0.05 ‰; 2 s.d., n = 4) agree well with other published values for the standards, and the calculated external precisions illustrate that sub-0.1‰ variations can be confidently resolved using our methods.

4.2 Granulite facies xenoliths

Silicon isotope data for the granulite facies xenoliths are given in Table 1 and plotted in Figure 1. Measurement uncertainty is given as both the 2 standard deviations (2 s.d.) and 95% standard error of the mean (95% s.e. = t × s.d./$(n)^{1/2}$, where t = inverse survival function of the Student's t-test at the 95% significance level and n-1 degrees of freedom).

The δ^{30}Si values for the xenoliths range from -0.43 to -0.15 ‰, with both suites displaying similar isotopic ranges (McBride δ^{30}Si = -0.40 to -0.15 ‰; Chudleigh δ^{30}Si = -0.43 to -0.20 ‰). These xenoliths, in particular the cumulate and restite lithologies, record some of the lightest "high temperature" terrestrial Si isotope compositions so far measured with modern high precision techniques (Fig. 1). The range of data for the McBride suite (~0.25 ‰) is similar to that seen in other igneous settings where there is also a wide range of SiO_2 concentrations (i.e. Hekla; Savage et al., 2011). There is also a good correlation between $\delta^{30}Si$ and SiO_2 (R^2 = 0.81) for the McBride samples (Fig. 2). Significantly, the Chudleigh samples do not show a similar correlation, and the range of SiO_2 is much more limited; this is most likely because these samples are not representative of equilibrium melt assemblages (see Section 5.3).

5. DISCUSSION

5.1 Silicon behaviour during high-grade metamorphism

Before we can use the xenolith $\delta^{30}Si$ data to discuss Si isotope behaviour during igneous processes, we must first assess any effect that syn- and post-eruptive alteration and/or high-grade metamorphism may have had on the primary Si concentration and isotopic signatures of the samples.

Low-temperature processes such as chemical weathering and secondary mineral formation result in relatively large degrees of Si isotopic fractionation compared to that seen during igneous processes (e.g. Ziegler et al., 2005a&b; Georg et al., 2009b; Opfergelt et al., 2012), which enrich the product in the lighter isotopes (~1.0‰ negative enrichments are not uncommon in secondary phases). It is unlikely that such processes have altered the primary Si isotopic compositions of the samples, as all weathered surfaces were removed before analysis, and no clay minerals were identified (Rudnick et al., 1986; Rudnick and Taylor, 1987; Teng et al., 2008). Also, Li, which is more fluid-mobile than Si, shows no isotopic evidence that chemical weathering has affected the isotopic composition of the xenoliths

(Teng et al., 2008). The rapid exhumation of the xenolith material will have limited alteration during eruption and also minimised retrograde metamorphism (Section 2). Lastly, there is no evidence for magmatic infiltration into sample material (Rudnick et al., 1986; Rudnick and Taylor, 1987).

Xenolith material in a basaltic magma is not at equilibrium, so diffusion of material between xenolith and melt could modify the primary chemical composition recorded by the sample. Large variations measured in Li isotopes in the Chudleigh and McBride xenolith samples are attributed to kinetic isotope fractionation as a result of diffusion between xenolith and magma, or between minerals (Teng et al., 2008). This work identified two samples whose mineral δ^7Li values are equal to their bulk δ^7Li composition and are, therefore, in isotopic equilibrium; these samples (BC and 83-131 from Chudleigh) have δ^{30}Si values that encompass the Si isotopic range for the xenoliths ($\delta^{30}Si_{BC}$ = -0.40 ± 0.04 ‰, $\delta^{30}Si_{83\text{-}131}$ = -0.23 ± 0.04 ‰; Table 1). Given that Li isotopes are much more susceptible to kinetic isotope effects than Si (Richter et al., 2003, 2009; Huang et al., 2010), we are confident that kinetic processes have not affected the Si isotopic composition of the xenoliths.

Finally, we assess the effect that granulite facies metamorphism has had on the bulk Si isotopic compositions of the xenolith. In the presence of a volatile phase, Si mobility increases with increasing temperature and, under such conditions, is mobile during metamorphism. Prograde metamorphism to granulite facies often involves dehydration (e.g. Stähle et al., 1987), which will reduce concentrations of fluid-mobile elements (such as Cs, U, B etc; Rudnick et al., 1985; Leeman et al., 1992) and could therefore affect Si. There are some granulite terranes where metasomatism via high temperature CO_2-rich fluids has mobilised Si (Stähle et al., 1987; Newton, 1989) but in many of these cases this is related to retrograde metamorphism, which is avoided by studying xenoliths. Nevertheless, a major metasomatic event that significantly altered the silica content of a xenolith may also have affected the primary δ^{30}Si.

In fact, in the original studies on both xenoliths suites, no evidence of silica metasomatism was noted (Rudnick et al., 1986; Rudnick and Taylor, 1987); comparing the silica contents of the xenoliths to the average SiO_2 of their respective protoliths, as well as their metamorphic assemblages, there is no evidence that Si has been lost or gained to any significant degree during metamorphism and/or residence in the lower crust. This is strongly supported by the Si isotopic compositions; the δ^{30}Si of the McBride xenoliths correspond to the average isotopic composition of their inferred protoliths. Mafic melts have δ^{30}Si of -0.32 to -0.28 ‰, identical within error to the δ^{30}Si BSE value and MORB/IAB averages (Savage et al., 2010) and the felsic xenoliths have δ^{30}Si values of -0.22 to -0.15 ‰, which are within the range measured for dacites, rhyolites and I-type granites (Savage et al., 2011 – see Fig. 1).

Given that the xenoliths from Chudleigh and McBride appear to record their primary Si isotopic compositions, it is evident that some Si isotopic heterogeneity exists in the lower continental crust. Although not as variable as the upper crust (which reflects the effect of low-temperature weathering and biogenic processes; Savage et al., 2012b), the range of δ^{30}Si values in the deep continental crust is comparable to that displayed by igneous rocks of the oceanic and upper continental crust and mantle (Fitoussi et al., 2009; Savage et al., 2010, 2011, 2012a; Armytage et al, 2011). We will now focus on interpreting the Si isotope variations in each xenolith suite in turn.

5.2 Silicon isotopic variation in the McBride xenolith suite

The McBride xenolith suite consists of samples that are genetically unrelated, in that there are no obvious correlations with major or trace elements (Rudnick and Taylor, 1987), hence there is little risk of cogenetic bias. Also, the samples yield a wide spread of zircon ages, sampling lower crust that has formation ages spanning millions of years (between

Proterozoic and Permo-Triassic; Rudnick and Williams, 1987). Lastly, the wide range of protolith lithologies represented by the McBride xenoliths contain most (if not all) of the rock types that are thought to comprise the lower crust (e.g. Rudnick and Fountain, 1995).

As mentioned in Section 5.1, there are striking similarities between the Si isotopic compositions of the melt-derived McBride xenoliths and those of their igneous counterparts measured by previous studies. This is demonstrated by the strong positive correlation between δ^{30}Si and SiO_2 (Fig. 2, $R^2 = 0.81$) which is collinear with the so-called "igneous array" (see Section 1; Savage et al., 2011), also plotted in Figure 2 for comparison. The fact that all of the meta-igneous xenolith data plot on or near to the "igneous array" is excellent evidence that the processes that control the Si isotopic composition of igneous rocks erupted at the surface are common to those controlling the composition of the lower crust; that is, the relative Si-O bond strengths, (controlled predominantly by polymerisation degree and chemical composition) between either a partial melt and restite, or a melt and crystallising phase(s), fractionate Si isotopes because it is energetically more favourable for the heavier isotopes to partition into phases with stronger Si-O bonds. This drives more silica-rich samples to heavier Si isotopic compositions (e.g. Grant, 1954; Méheut et al., 2009; Savage et al., 2011). This strong relationship also suggests that samples do not need to be cogenetic to fall on the "igneous array"; rather, they simply need to represent equilibrium melt compositions.

In detail, the mafic xenolith samples 85-100 and 85-120 have δ^{30}Si values (-0.32 to -0.28 ‰); identical, within error, to those of MORB, IAB and mantle-derived suites (Savage et al., 2010). These samples probably represent basaltic magma added to the lower crust by underplating (Rudnick, 1990). Simplistically, the Si isotope composition of the majority of the McBride samples can be explained by crystallisation of isotopically light olivine or pyroxene (Fig. 1) from this basaltic material to generate a felsic melt with a heavy δ^{30}Si signature (samples 83-160 and 83-162), leaving a cumulate enriched in the lighter Si isotopes. This is shown by a simple fractional crystallisation model in Figure 2, using the average composition of the two mafic melt xenoliths as the starting composition (SiO_2 = 52 wt. %; $\delta^{30}Si$ = -0.30‰) and a bulk $\Delta^{30}Si_{solid-melt}$ value of -0.125‰ (as calculated for the “igneous array” by Savage et al., 2011). The model fit to the xenolith data (and also the igneous array) is good, and suggests that ~80% crystallisation is required to generate the felsic melts, a plausible figure. Using mass balance (and assuming a closed system) the cumulate compositions have been calculated for each 10% crystallisation step. The array of compositions, also shown in Figure 2, is in broad agreement with the restite data. Although these samples are not strictly cumulates, these isotopically light restites (samples 83-159 and 85-114) could be generated, by partial melting of a basaltic protolith, creating a isotopically heavy feldspathic melt and a relatively light refractory restite. This is not to suggest that this xenolith suite is cogenetic; rather the predictability of Si isotopes during magmatic differentiation is such that even unrelated samples can be easily modelled using a single bulk $\Delta^{30}Si_{solid-melt}$ value.

Although this simple framework can adequately explain the Si isotopic variation, other isotope data indicate that petrogenesis of the McBride xenolith suite was not simply closed-system magmatic differentiation. In particular, the Sr, Nd and O isotope compositions of the xenolith suite do not lay within the ranges for mantle material (Fig. 3 & 4), suggesting that a significant amount of assimilation of an evolved crustal source occurred during petrogenesis (Rudnick, 1990; Kempton and Harmon, 1992). It is therefore pertinent to assess whether assimilation may have altered the Si isotope composition of these xenoliths.

5.2.1 $\delta^{30}Si$ vs. $^{87}Sr/^{86}Sr$

No correlation exists between $\delta^{30}Si$ and initial (age corrected) $^{87}Sr/^{86}Sr$ and εNd (Fig.

3; Nd not shown). This is good evidence that assimilation of an isotopically evolved crustal component has not resolvably affected the Si isotope composition of the xenoliths.

Previous work on the McBride xenoliths used AFC processes (assimilation and fractional crystallisation) to explain the Sr and Nd isotopic variations (Rudnick, 1990). Here, Sr and Nd isotope compositions were successfully modelled using an elevated r value (where r is the ratio of assimilant flux to cumulate formation) of 0.9, and minor fractional crystallisation (f = 0.9-0.95, where f is fraction of melt remaining). Figure 3 shows the r = 0.9 AFC trajectory in $\delta^{30}Si$ vs. $^{87}Sr/^{86}Sr$ space, calculated after DePaolo (1981), employing a starting melt (“B”) based on mantle-derived basalt ($\delta^{30}Si$ = -0.32‰) and assimilant based on the composition of metasediment xenolith 83-157 ($\delta^{30}Si$ = -0.31‰; end member compositions, D values and bulk $\Delta^{30}Si_{solid\text{-}melt}$ are given in Electronic Annexe EA-1). In this case, AFC (r=0.9; f=0.95) successfully predicts the composition of the mafic xenoliths, but fails to reach the heavier $\delta^{30}Si$ compositions of the felsic samples. This is because the meta-sediment $\delta^{30}Si$ is unfractionated relative to the mafic melt.

One way to explain this is to invoke a separate AFC trend for the felsic samples, as these xenoliths are not cogenetic. A good match to the data is returned using a much lower r value (0.2) and larger melt depletion (~70%); however, such low r values are physically unlikely for the hot lower crust, where rocks are already near melting (James, 1981). More probable, the felsic samples can be easily explained via partial melting of a basaltic source, which earlier formed along the AFC r=0.9 trend. Partial melting would fractionate $\delta^{30}Si$ parallel to the “igneous array” line in Figure 3 but would not affect $^{87}Sr/^{86}Sr$, resulting in a melt enriched in ^{30}Si and leaving isotopically light restites.

A final possibility to consider is that the McBride xenoliths all derived from an already enriched mantle (i.e., source rather than crustal contamination). This is demonstrated by the two component mixing line in Figure 3, where between 20 and 40% contamination of an isotopically enriched end member is required to explain the $^{87}Sr/^{86}Sr$ isotope compositions of the xenoliths. However, this is unsupported by data from primitive basalts and mantle xenoliths in the region, which indicate that the mantle below northern Queensland has a primitive composition (Ewart et al., 1988).

5.2.2 $\delta^{30}Si$ vs. $\delta^{18}O$

Kempton and Harmon (1992) noted that O isotopes do not correlate well with elemental or radiogenic isotope compositions in the McBride xenolith suite. This was interpreted to be a result of the comparatively ancient pre-existing continental crust at this locality, which, over geological time, has developed a variety of isotopically and elementally heterogeneous crustal components. It is surprising then, that a plot of $\delta^{30}Si$ against $\delta^{18}O$ for the McBride suite reveals a good correlation with O isotopes (Fig. 4).

Oxygen isotopes are fractionated by igneous processes to heavier compositions, but not to the degree of isotope enrichment seen in the McBride suite (<1‰ variations between basaltic and rhyolitic material are typical; Taylor and Sheppard, 1986). The oxygen isotope data for the McBride samples are all at least 2.5‰ heavier than the canonical mantle value ($\delta^{18}O$ = +5.5‰, Mattey et al., 1994), indicating the presence of a source that has been affected by low temperature chemical weathering (e.g. Taylor and Sheppard, 1986). Even though there is good evidence to suggest that Si isotopes have not been resolvably affected by crustal contamination (due to the apparently unfractionated nature of the metasedimentary material in this locality), the $\delta^{30}Si$ vs. $\delta^{18}O$ correlation merits comment, specifically: can we model this relationship in terms of igneous processes?

As in Figure 3, we have attempted to model the data as a function of AFC processes. Figure 4a shows a set of AFC trajectories in $\delta^{30}Si$ vs. $\delta^{18}O$ space, with a mantle-derived starting melt identical to “B” in Figure 3 ($\delta^{30}Si$ = -0.32‰, $\delta^{18}O$ = +5.5‰). In this case, the assimilant (“A”) used in this model is dissimilar to that shown in Figure 3. This is because, as noted by Rudnick (1990), the high degrees of assimilation of metasedimentary material required by the isotope compositions of the McBride suite should be reflected in their major elemental composition – which is not the case. To solve the assimilant problem, Kempton and Harmon (1992) suggest that the contaminant is “mafic restite remaining from a metasedimentary or δ^{18}O-enriched metaigneous protolith after granite genesis,” which could be assimilated in large amounts without significantly altering the elemental composition of a mafic melt. Hence, a putative restite was utilised as the assimilant, with a slightly lighter δ^{30}Si than the metasediment (-0.37‰, averaged from the restite xenolith analyses), and the most extreme δ^{18}O value (+13.2‰) measured from the McBride suite (see Electronic Annexe EA-1).

As in Figure 3, the AFC (r=0.9, f=0.95) curve successfully predicts the more mafic xenolith compositions, however, the felsic xenoliths cannot be explained by partial melting of the mafic samples. This is show by the arrow in Figure 4a, which does not overlap the high enriched O isotope composition of these samples. Although partial melting of material whose source is modelled at lower f value (~0.85) along this curve could explain the O isotope data, the melt would be too enriched in ^{87}Sr (see Fig. 3).

Also, in contrast to the δ^{30}Si-^{87}Sr/^{86}Sr data, an AFC trend with lower r (0.2) and high melt depletion values does not pass through any of the data. This could indicate that the composition of the assimilant is incorrect; however, assigning component “A” with a heavier δ^{30}Si composition results in the model predicting the felsic samples but not the mafic xenoliths – the same is found if the assimilant is assigned a much heavier O isotope composition, using the r=0.2 curve. It appears, therefore, extremely difficult to modelling the δ^{30}Si data δ^{18}O of the McBride xenoliths using AFC processes and a mantle-derived source.

A final adaptation of the model is to invoke that the starting melt was already ^{18}O-enriched before differentiation began. This could be generated a number of ways, either by source contamination resulting in an enriched mantle (although there is little evidence for this, see above), assimilation *without* fractional crystallisation of an evolved end-member (physically unlikely) or, similar to the "restite" model of granite genesis proposed by Chappell (e.g. Chappell et al, 1987), concomitant melting of a solid mixture of both primitive and evolved components. Nevertheless, a mixing line between a mantle-derived basalt and the restite contaminant (plotted in Figure 4b) gives a putative array of melt compositions; using the results from the model in Figure 3, we have used a mixture of 30% restite and 70% basalt as the starting melt ("M" in Fig. 4b; $\delta^{30}Si = -0.33$, $\delta^{18}O = +8.0‰$). Finally, AFC trends were calculated using "M" as the starting melt composition, again for different values of r. These models require r to be elevated, but values between 0.4 and 0.6, rather than 0.9, adequately explain both the Si and O isotope data for the McBride suite. These curves, all require high degrees of melt depletion (f = 0.2-0.4) in contrast to those of Rudnick (1990), although this may no longer be a problem given that the assimilant is mafic restite, rather than metasediment. On the basis of coupled $\delta^{30}Si$-$\delta^{18}O$ analyses, if appears that petrogenesis of the McBride xenoliths involved assimilation of an evolved crustal source into an already previously enriched, differentiating melt phase.

5.3 Silicon isotopic variation in the Chudleigh xenolith suite

In comparison to the variety of lithologies represented by the McBride suite, the Chudleigh xenoliths are all mafic cumulates (SiO_2 between 49.6 and 51.0 wt %), with isotopic compositions ranging in $\delta^{30}Si$ between -0.43 and -0.20 ‰. This is a much larger range than would be predicted if the Chudleigh xenolith protoliths represented mafic melts (see Fig. 2), so it seems likely that this large variation is a result of the cumulate-derived mineralogy and composition of the xenoliths. Note that the Chudleigh xenoliths display much more mantle-like $\delta^{18}O$, $^{87}Sr/^{86}Sr$ and εNd (Fig. 3 and 4), indicating that crustal assimilation was either more limited than for the McBride samples, or that the crustal end-member was much less evolved.

In Section 1 we hypothesise that lower crustal igneous cumulates should have light Si isotope compositions relative to BSE, as a result of the enrichment of heavy Si isotopes in the melt phase during magmatic differentiation. In fact, only two cumulates are isotopically lighter than BSE, with the majority lying within the range of effusive igneous rocks, shown in Figure 1. The Chudleigh cumulates have significant modal abundances of plagioclase as well as olivine and pyroxene – plagioclase is typically isotopically heavier than BSE when forming from a mafic melt (Fig. 1), which would serve to balance out the lighter mafic phases.

This mineralogical control is demonstrated by a negative correlation between $\delta^{30}Si$ and Mg# (Mg# = molar MgO/[MgO + 0.85 × FeO_{total}]; Fig. 5a; $R^2 = 0.63$, excluding sample 83-112 whose Mg# is much lower due to cumulate oxide phases, Rudnick et al., 1986). Furthermore, there is a positive correlation between $\delta^{30}Si$ and Eu/Eu* (Fig. 5b, $R^2 = 0.52$). Elevated Mg# can be an indication of large primary proportions of olivine and pyroxene (Mg-rich phases) and elevated Eu/Eu* (defined as $2\times Eu_N/[Sm_N\times Gd_N]^{0.5}$ where subscript N denotes that the concentrations are normalised to chondritic values) identifies the presence of cumulate plagioclase in a sample. Therefore, the Si isotopic composition of the Chudleigh xenoliths appear to be controlled by the ratio of olivine and pyroxene to plagioclase in the cumulate, with the most negative $\delta^{30}Si$ values corresponding to the largest proportions of Mg-rich phases. There is also a strong negative correlation between $\delta^{30}Si$ and CIPW normative diopside (not shown, $R^2 = 0.78$). Taken with the better correlation for Mg# than Eu/Eu*, this provides evidence that the abundance of ferromagnesian phases, more specifically pyroxene, is the dominant control over Si isotopes in this cumulate system.

Using the Skaergaard mineral separate data (Fig. 1, Savage et al., 2011) and the CIPW normative mineral compositions given in Rudnick et al. (1986), the predicted δ^{30}Si value of the xenoliths can be calculated, assuming that the cumulates formed from a mafic melt. These values are given as δ^{30}Si(m) in Table 1. While the range of predicted values (δ^{30}Si = -0.39 to -0.24 ‰) is very close to the measured range, there is poor correspondence between the predicted and actual isotopic composition for each xenolith sample. Either the fractionation factors deduced from the mineral separate data are not universally applicable, or another process, other than cumulate formation, may be affecting the Si composition of these xenoliths.

Although the former cannot be discounted, major element characteristics provide evidence for the latter. Rudnick et al. (1986) state that the variation in Mg# displayed by the Chudleigh xenoliths is too large to be solely affected by the proportions of ferromagnesian phases in the sample. They suggest that these data also reflect variations in the composition of the coexisting melt; specifically, that those xenoliths with low Mg# have equilibrated with a more evolved (Si-rich) melt. Assuming that a more Si-rich melt will have a heavier Si isotopic composition, then cumulates deriving from this phase should be correspondingly enriched in the heavier isotopes. This may be too simplistic, however, as the Si isotopic composition of a mineral phase is likely to be controlled by the relative bonding environments of Si between the phase and the melt (Méheut et al., 2009; Savage et al., 2011) and an increase in the polymerisation degree of a melt will result in variations in the mineral-melt fractionation factors. Nevertheless, the data provide evidence that the Si isotopic compositions of the Chudleigh xenoliths are controlled predominantly by mineralogy, with subtle isotopic variations introduced by compositional changes in the coexisting melt phase. On the basis of these data, it appears that the lower continental crust is not a hidden light reservoir for Si isotopes.

5.4 Silicon isotopic composition of the lower and middle continental crust

There are a number of ways with which the xenolith data can be used to calculate a Si isotope composition for the LCC. The first is to take a simple arithmetic mean, which gives a value of $\delta^{30}Si = -0.29 \pm 0.15$ ‰ (2 s.d.; Table 2); this value is identical to the canonical $\delta^{30}Si$ BSE value (Savage et al., 2010) and reflects the overall mafic composition of the this region, and also that cumulates are not always enriched in the light Si isotopes, as was originally suggested. The relatively large errors on the mean reflect the range of isotopic compositions that are displayed in the lower crust. A second method is to take a weighted mean, using the ratio of a sample's SiO_2 content against that of the LCC (53.4 wt.%, Rudnick and Gao, 2003) as the weighting parameter. This gives a similar value, of $\delta^{30}Si = -0.28 \pm 0.15$ ‰ (2 s.d.; Table 2), because most of the xenoliths analysed are also mafic.

The final way is more involved, and uses the average lithological compositions of the LCC, as estimated by Rudnick and Fountain (1995), and average Si isotope compositions for each lithology, to calculate a bulk estimate. This method is arguably the most robust, as bulk xenolith composition and the lithologies represented vary considerably between continents (e.g. Condie and Selverstone, 1999; Villaseca et al., 1999; Liu et al., 2001) and so using the first two methods, rather than calculating a global average, could bias the calculation toward the Australian lower crust.

This method starts by providing average values for the mafic, intermediate (andesitic), felsic and sedimentary components of the crust. The felsic average was taken from the two xenoliths that represent felsic melts from McBride, and the sedimentary average was taken from measurements of shales and loess (Savage et al., 2012b). This estimate of $\delta^{30}Si = -0.32 \pm 0.40$ ‰ (2 s.d.) has large error bars, reflecting the broader range of data for sediments compared to igneous rocks, although the mean value is very close to the one meta-sediment analysed in this study (83-157). The mafic average is more complicated, because, as is shown above, mafic cumulates have a much larger range of $\delta^{30}Si$ values than mafic melts – therefore it is important to calculate a value that reflects the ratio of cumulate-derived to melt-derived material in the lower crust. To estimate this, the global compilation of granulite facies xenolith data of Kempton and Harmon (1992) was used to infer cumulate:melt:restite populations; from this estimate, of the mafic xenoliths, 52% are melt-, 41% are cumulate-, and 6% are restite-derived. This results in a mafic cumulate average of $\delta^{30}Si$ = -0.30 ± 0.07 ‰ (2 s.d.). Finally, the intermediate average is taken as the mean of the mafic and felsic averages, viz. $\delta^{30}Si$ = -0.24 ± 0.16 ‰ (2 s.d.).

Table 2 shows the results for a number of different lower crustal types, with different lithological proportions. There is very little variation between the calculated lower crustal compositions, with all values ($\delta^{30}Si$ ranging from -0.30 to -0.26 ‰) close to the simple and weighted means. The consistency of all of these values gives confidence that our original, simple mean value of $\delta^{30}Si$ = -0.29 ± 0.15 ‰ (2 s.d.) is a good estimate of the Si isotope composition of the lower crust. The precision on this estimate reflects the Si isotope variability in the lower crust; however, the consistency of the average $\delta^{30}Si$ calculated using various methods suggests that this value is better constrained than the precision indicates. Using a 95% standard error reflects the precision of this mean at the 95% confidence level, and gives a more precise estimate of $\delta^{30}Si$ = -0.29 ± 0.04 ‰ (95% s.e.). As an aside, the 2 s.d. calculated using the various average $\delta^{30}Si$ lower crust compositions given in Table 2 is even smaller (± 0.03 ‰).

Note that this value is identical to that of BSE (Savage et al., 2010). It was predicted that, because mafic mineral phases have relatively light Si isotopic compositions, the process of fractional crystallisation would create cumulate material with correspondingly light compositions; therefore, the cumulate-dominated lower crust should also be isotopically light relative to basalt and BSE. Here this hypothesis is disproven, as cumulate lithologies display a wide range of Si isotope compositions, comparable to those of other igneous rocks (Fig. 1); as such, the LCC has an isotopic composition that is more heterogeneous but almost identical on average to the mantle.

The composition of the middle crust can also be estimated using the weighted mean method and the lithological method as described above; these estimates are also presented in Table 2. This method relies on some assumptions and a more robust estimate would make use of Si isotope analyses of middle crustal lithologies (i.e. granulite and amphibolite facies terranes), however, the exercise can give with a first order estimate. The weighted average value for the middle crust is $\delta^{30}Si$ = -0.23 ± 0.15 ‰; 2 s.d. (± 0.04 ‰; 95% s.e.). This is slightly heavier than both the lower and upper crust and reflects the predominantly andesitic composition, and paucity of weathered sedimentary material, of this region.

6. CONCLUSIONS

Granulite xenolith samples from the Chudleigh and McBride volcanic provinces, Australia, provide novel insights into how the Si isotope system behaves during igneous processes, specifically cumulate formation and magmatic differentiation when crustal assimilation is taking place. In addition, these samples also record the Si isotopic composition of the deep continental crust.

Sixteen samples have been analysed, which display a range of isotopic data ($\delta^{30}Si$ = -0.43 to -0.15 ‰) comparable to that measured elsewhere in igneous rocks, from the upper crust, oceanic crust and mantle. For the McBride xenolith suite, magmatic differentiation appears to be the major factor controlling Si isotope composition, whereby increasing SiO_2

content is accompanied by a concomitant increase in the heavier isotopes. This phenomenon is observed globally, in many other magmatic systems (e.g. Savage et al., 2011). The McBride data provides good evidence that samples do not need to be cogenetic for their Si isotope compositions to exhibit this relationship; rather, they simply need to represent equilibrium melt compositions, and therefore this relationship appears to be a fundamental property of the Si isotope system.

Silicon isotope analysis has also provided insights into the petrogenesis of the McBride xenoliths. On the basis of Si-Sr isotope systematics, petrogenesis of the McBride xenoliths can be explained using a mantle-derived basaltic source that undergoes AFC to form the mafic xenoliths; further partial melting of this material generates the felsic and restite samples. This model does not, however, agree with the O isotope data; specifically, a good correlation between δ^{30}Si and δ^{18}O is explained by AFC processes acting on a previously-enriched source melt (relative to primitive mantle), containing ~30% of an evolved component.

The cumulate-derived Chudleigh xenoliths have Si isotope compositions ranging from δ^{30}Si = -0.43 to -0.20 ‰. Good relationships between δ^{30}Si and Mg#, Eu anomaly and CIPW normative diopside content provide strong evidence that the Si isotope composition of these samples is predominantly controlled by the mineralogy of individual cumulates. In particular, phases that have higher Mg# tend to concentrate the lighter isotopes, therefore a cumulate that is olivine or pyroxene-rich will have a lighter isotopic composition. The range of Si isotope compositions in cumulates is similar to that displayed by effusive igneous material; on this basis, the lower continental crust is not a hidden light reservoir for Si isotopes.

The average Si isotopic compositions of the lower and middle continental crust have been calculated using the xenolith data, combined with a number of weighting methods. The methods all give estimates that agree with one another, so we are confident that our compositions are representative. These values are: $\delta^{30}Si$ = -0.29 ± 0.04 ‰ (95% s.e.) for the LCC, and; $\delta^{30}Si$ = -0.23 ± 0.04 ‰ (95% s.e.) for the MCC. These values are almost identical to the composition of the Bulk Silicate Earth, indicating that only minor isotopic fractionation occurs as a result of continental crust formation.

Acknowledgements: The authors would like to thank Roberta Rudnick, who kindly provided all the samples analysed in this study as well as reviewing an early version of this manuscript. This work benefited immensely from scientific discussion with Ros Armytage, Julie Prytulak and Kevin Burton. Expert editorial advice and incisive reviews and comments from three anonymous reviewers and Mark Harrison greatly improved the manuscript. The authors would also like to acknowledge the invaluable technical assistance and expertise provided by Steve Wyatt, Nick Belshaw and Teo Krastev at the University of Oxford. This work was funded by a NERC CASE studentship supported by Nu Instruments with additional analytical costs by an ERC Advanced Fellowship to A.H.

REFERENCES

Abraham K., Opfergelt S., Fripiat F., Cavagna A., de Jong J. T. M., Foley S. F., André L. and Cardinal D. (2008) δ^{30}Si and δ^{29}Si Determinations on USGS BHVO-1 and BHVO-2 Reference Materials with a New Configuration on a Nu Plasma Multi-Collector ICP-MS. *Geostand. Geoanal. Res.* **32,** 193-202.

Allen M. A. (1998) Comminution of geological samples using Syalon based milling vessels: comparison with established sample preparation methods. Anal. Commun. **35**, 75-78.

Armytage R. M. G., Georg R. B., Savage P. S., Williams H. M. and Halliday A. N. (2011) Silicon isotopes in meteorites and planetary core formation. *Geochim. Cosmochim. Acta* **75,** 3662-3676.

Basile-Doelsch I. (2006) Si stable isotopes in the Earth's surface: A review. *J. Geochem. Explor.* **88,** 252-256.

Bohlen S. R. and Mezger K. (1989) Origin of granulite terranes and the formation of the lowermost continental crust. *Science* **244,** 326-329.

Chakrabarti R. and Jacobsen S. B. (2010) Silicon isotopes in the inner Solar System: Implications for core formation, solar nebular processes and partial melting. *Geochim. Cosmochim. Acta* **74,** 6921-6933.

Chappell B. W., White A. J. R. and Wyborn D. (1987) The Importance of Residual Source Material (Restite) in Granite Petrogenesis. *J. Petrol.* **28 (6)**, 111-1138.

Condie K. C. and Selverstone J. (1999) The crust of the Colorado Plateau: New views of an old arc. *J. Geol.* **107,** 387-397.

Dawson J. B. (1977) Sub-cratonic crust and upper mantle models based on xenolith suites in kimberlite and nephelinitic diatremes. *J. Geol. Soc.* **134,** 173-184.

De la Rocha, C. L., Brzezinski, M. A. and DeNiro, M. J. (2000). A first look at the distribution of the stable isotopes of silicon in natural waters. . *Geochim. Cosmochim. Acta* **64**, 2467-2477.

DePaolo D. J. (1981) Trace element and isotopic effects of combined wallrock assimilation and fractional crystallization. *Earth Planet. Sci. Lett.* **53,** 189-202.

Ding T., Jiang S., Wan D., Li Y., Li J., Song H., Liu Z. and Yao X. (1996) *Silicon Isotope Geochemistry.* Geological Publishing House, Beijing, China.

Douthitt C. B. (1982) The geochemistry of the stable isotopes of silicon. *Geochim. Cosmochim. Acta* **46,** 1449-1458.

Ewart, A.J., Chappell, B.W. and Menzies, M.A., 1988. An overview of the geochemical and isotopic characteristics of the eastern Australian Cainozoic volcanic provinces. *J. Petrol., Spec. Lithosphere Iss.,* 225-273.

Fitoussi C., Bourdon B., Kleine T., Oberli F. and Reynolds B. C. (2009) Si isotope systematics of meteorites and terrestrial peridotites: implications for Mg/Si fractionation in the solar nebula and for Si in the Earth's core. *Earth Planet. Sci. Lett.* **287,** 77-85.

Fountain D. M. and Salisbury M. H. (1981) Exposed cross-sections through the continental crust: implications for crustal structure, petrology, and evolution. *Earth Planet. Sci. Lett.* **56,** 263-277.

Georg R. B., Reynolds B. C., Frank M. and Halliday A. N. (2006) New sample preparation techniques for the determination of Si isotopic compositions using MC-ICPMS. *Chem. Geol.* **235,** 95-104.

Georg, R. B., West, A. J., Basu, A. R., Halliday, A.N. (2009a) Silicon fluxes and isotope composition of direct groundwater discharge into the Bay of Bengal and the effect on the global ocean silicon isotope budget. *Earth Planet. Sci. Lett.* **283,** 67-74.

Georg R. B., Zhu C., Reynolds B. C. and Halliday A. N. (2009b) Stable silicon isotopes of groundwater, feldspars, and clay coatings in the Navajo Sandstone aquifer, Black Mesa, Arizona, USA. *Geochim. Cosmochim. Acta* **73,** 2229-2241.

Grant F. S. (1954) The geological significance of variations in the abundances of the isotopes of silicon in rocks. *Geochim. Cosmochim. Acta* **5,** 225-242.

Holbrook W. S., Mooney W. D. and Christensen N. I. (1992) The seismic velocity structure of the deep continental crust. *Continental Lower Crust,* 1-43.

Huang F., Chakraborty P., Lundstrom C. C., Holmden C., Glessner J. J. G., Kieffer S. W. and Lesher C. E. (2010) Isotope fractionation in silicate melts by thermal diffusion. *Nature* **464,** 396-400.

James, D.E. (1981) The combined use of oxygen and radiogenic isotopes as indicators of crustal contamination. *Annu. Rev. Earth Planet. Sci.,* **9**, 311-344.

Kempton P. D. and Harmon R. S. (1992) Oxygen isotope evidence for large-scale hybridization of the lower crust during magmatic underplating. *Geochim. Cosmochim. Acta* **56,** 971-986.

Leeman, W.P., Sisson, V.B. and Reid, M.R. (1992) Boron Geochemistry of the Lower Crust - Evidence from Granulite Terranes and Deep Crustal Xenoliths. *Geochim. Cosmochim. Acta* **56**, 775-788

Liu Y., Gao S., Jin S., Hu S., Sun M., Zhao Z. and Feng J. (2001) Geochemistry of lower crustal xenoliths from Neogene Hannuoba Basalt, North China Craton: Implications for petrogenesis and lower crustal composition. *Geochim. Cosmochim. Acta* **65,** 2589-2604.

Mattey D, Lowry D and Macpherson C (1994) Oxygen isotope composition of mantle peridotite. *Earth Planet. Sci. Lett.* **128 (3-4),** 231-241.

Méheut M., Lazzeri M., Balan E. and Mauri F. (2009) Structural control over equilibrium silicon and oxygen isotopic fractionation: A first-principles density-functional theory study. *Chem. Geol.* **258,** 28-37.

Newton R. C. (1989) Metamorphic fluids in the deep crust. *Ann. Revi. Earth Planet. Sci.* **173,** 85-412.

Opfergelt S., Georg R. B., Delvaux B., Cabidoche Y.-M., Burton K. W. and Halliday A. N. (2012) Silicon isotopes and the tracing of desilication in volcanic soil weathering sequences, Guadeloupe. *Chem. Geol.* **326-327,** 113-122.

Reynolds B. C., Aggarwal J., André L., Baxter D., Beucher C., Brzezinski M. A., Engström E., Georg R. B., Land M., Leng M. J., Opfergelt S., Rodushkin I., Sloane H. J., Van Den Boorn S. H. J. M., Vroon P. Z. and Cardinal D. (2007) An inter-laboratory comparison of Si isotope reference materials. *J. Anal. Atom. Spectrom.* **22,** 561-568.

Richter F. M., Davis A. M., DePaolo D. J. and Watson E. B. (2003) Isotope fractionation by chemical diffusion between molten basalt and rhyolite. *Geochim. Cosmochim. Acta* **67,** 3905-3923.

Richter F. M., Dauphas N. and Teng F-Z. (2009) Non-traditional fractionation of non-traditional isotopes: Evaporation, chemical diffusion and Soret diffusion. *Chem. Geol.* **258,** 92-103.

Rudnick R. L. (1990) Nd and Sr isotopic compositions of lower-crustal xenoliths from north Queensland, Australia: Implications for Nd model ages and crustal growth processes. *Chem. Geol.* **83,** 195-208.

Rudnick R. L. and Fountain D. M. (1995) Nature and composition of the continental crust: A lower crustal perspective. *Rev. Geophys.* **33,** 267-309.

Rudnick R. L. and Taylor S. R. (1987) The composition and petrogenesis of the lower crust: A xenolith study. *J. Geophys. Res.* **92,** 13981-14005.

Rudnick R. L. and Taylor S. R. (1991) Petrology and geochemistry of lower crustal xenoliths from northern Queensland and inferences on lower crustal composition. In (Drummond, B., ed) The Australian Lithosphere, *Spec. Pub. Geol. Soc. Australia* **17** 189-208.

Rudnick R. L. and Williams I. S. (1987) Dating the lower crust by ion microprobe. *Earth Planet. Sci. Lett.* **85,** 145-161.

Rudnick R. L. and Goldstein S. L. (1990) The Pb isotopic compositions of lower crustal xenoliths and the evolution of lower crustal Pb. *Earth Planet. Sci. Lett.* **98,** 192-207.

Rudnick R. L. and Gao S. (2003) Composition of the continental crust. *Treatise on Geochemistry* **3,** 1-64.

Rudnick, R.L., McLennan, S.M. and Taylor, S.R. (1985) Large ion lithophile elements in high-pressure granulite facies terrains. *Geochim. Cosmochim. Acta* **49**: 1645-1655.

Rudnick R. L., McDonough W. F., McCulloch M. T. and Taylor S. R. (1986) Lower crustal xenoliths from Queensland, Australia: Evidence for deep crustal assimilation and fractionation of continental basalts. *Geochim. Cosmochim. Acta* **50,** 1099-1115.

Saal A. E., Rudnick R. L., Ravizza G. E. and Hart S. R. (1998) Re-Os isotope evidence for the composition, formation and age of the lower continental crust. *Nature* **393,** 58-61.

Savage P. S., Georg R. B., Armytage R. M. G., Williams H. M. and Halliday A. N. (2010) Silicon isotope homogeneity in the mantle. *Earth Planet. Sci. Lett.* **295,** 139-146.

Savage P. S., Georg R. B., Williams H. M., Burton K. W. and Halliday A. N. (2011) Silicon isotope fractionation during magmatic differentiation. *Geochim. Cosmochim. Acta* **75,** 6124-6139.

Savage P. S., Georg R. B., Williams H. M., Turner S., Halliday A. N., Chappell B. W. (2012a) The silicon isotope composition of granites, *Geochim. Cosmochim. Acta* **92**, 184-202.

Savage P. S., Georg R. B., Williams H. M., Halliday A. N (2012b) A silicon isotopic record of long term changes in continental weathering. *Min. Mag.,* **76(6),** 2329.

Stähle H. J., Raith M., Hoernes S. and Delfs A. (1987) Element mobility during incipient granulite formation at Kabbaldurga, Southern India. *J. Petrol.* **28,** 803-834.

Taylor H. P. and Sheppard S. M. F. Igneous rock: I, Processes of isotopic fractionation and isotope systematics. *Reviews in Mineralogy and Geochemistry*, 1986, **v. 16**, p. 227-271

Teng F. -Z., Rudnick R. L., McDonough W. F., Gao S., Tomascak P. B. and Liu Y. (2008) Lithium isotopic composition and concentration of the deep continental crust. *Chem. Geol.* **255,** 47-59.

Tréguer P., Nelson D. M., Van Bennekom A. J., DeMaster D. J., Leynaert A. and Quéguiner B. (1995) The silica balance in the world ocean: A reestimate. *Science* **268,** 375-379.

Van Den Boorn S. H. J. M., Vroon P. Z. and Van Bergen M. J. (2009) Sulfur-induced offsets in MC-ICP-MS silicon-isotope measurements. *J. Anal. At. Spectrom.* **24,** 1111-1114.

Villaseca C., Downes H., Pin C. and Barbero L. (1999) Nature and composition of the lower continental crust in Central Spain and the granulite-granite linkage: Inferences from granulitic xenoliths. *J. Petrol.* **40,** 1465-1496.

Weyer S. and Schwieters J. (2003) High precision Fe isotope measurements with high mass resolution MC-ICPMS. *Int. J. Mass Spectrom.* **226**, 355-368.

Zambardi T. and Poitrasson F. (2011a) A combined Earth-Moon Si isotopes model to track rocks petrogenesis. *Min. Mag.* **75(3),** 2243.

Zambardi T. and Poitrasson F. (2011) Precise Determination of Silicon Isotopes in Silicate Rock Reference Materials by MC-ICP-MS. *Geostand. Geoanal. Res.* **35,** 89-99.

Ziegler K., Chadwick O. A., Brzezinski M. A. and Kelly E. F. (2005a) Natural variations of δ^{30}Si ratios during progressive basalt weathering, Hawaiian Islands. *Geochim. Cosmochim. Acta* **69,** 4597-4610.

Ziegler K., Chadwick O. A., White A. F. and Brzezinski M. A. (2005b) δ^{30}Si systematics in a granitic saprolite, Puerto Rico. *Geology* **33,** 817-820.

Ziegler K., Young E. D., Schauble E. A. and Wasson J. T. (2010) Metal-silicate silicon isotope fractionation in enstatite meteorites and constraints on Earth's core formation. *Earth Planet. Sci. Lett.* **295,** 487-496.

FIGURE CAPTIONS

Figure 1: $\delta^{30}Si$ compositions of various volcanic lithologies from Hekla volcano, Iceland, as well as silicate mineral separates, taken from Savage et al. (2011); CPX = clinopyroxene. Also shown is the Si isotope composition of Bulk Silicate Earth, taken from Savage et al. (2010; grey bar is 2sd uncertainty on the average). Data from this study is plotted below the dotted line, separated by protolith lithology – in general, the restite and cumulate material range to lighter $\delta^{30}Si$ values, whereas the felsic melts are isotopically heavy. Error bars are 2se.

Figure 2: Graph of $\delta^{30}Si$ versus SiO_2 for the Chudleigh (white symbols) and McBride (grey symbols) xenolith data (error bars are 95% s.e.). Also plotted for comparison is the "igneous array" (crosses and trend line), as defined by Savage et al. (2011). The McBride xenoliths representing melt protoliths fall on or near the igneous trend, and so exhibit a good positive relationship between $\delta^{30}Si$ and SiO_2. The Chudleigh samples do not exhibit this relationship, as they are not representative of equilibrium melt assemblages. Dotted line represents a putative fractional crystallisation trend for the McBride samples, using a bulk D_{Si} of 0.8 and a bulk $\Delta^{30}Si_{solid\text{-}melt}$ of -0.125‰ (tick marks are 10% crystallisation). The dashed line represents the cumulate compositions, calculated by mass balance for each 10% crystallisation step.

Figure 3: Graph of $\delta^{30}Si$ versus $^{87}Sr/^{86}Sr$ and for the Chudleigh and McBride xenoliths (symbols and error bars as for Figure 2). Strontium isotopic data for the McBride samples are age corrected; this correction has not been made for the Chudleigh suite but makes little difference, as Rb/Sr ratios are extremely low; as such, there has been insubstantial ^{87}Sr ingrowth. Dotted lines are AFC trends calculated after DePaolo (1981) for different r values

(cross marks are 10% melt removal steps), starting from a mantle-derived basaltic melt (“B”) employing the metasedimentary xenolith as the contaminant (end-member compositions are given in Electronic Annexe EA-1). A line joining “B” to “R” (rhyolite) is analogous to the “igneous array” as plotted in Figure 2, trends parallel to this originating from the r=0.9 AFC curve define magmatic differentiation of an enriched source (fractionating Si without affecting $^{87}Sr/^{86}Sr$).

Figure 4: Graph of $\delta^{30}Si$ versus $\delta^{18}O$ for the Chudleigh and McBride xenoliths (symbols and error bars as for Figure 2; Chudleigh data only shown in (a) for clarity). a) Trend line is for the McBride data only and shows the good relationship between the two isotope systems. Lines are AFC trends calculated after DePaolo (1981) for different r values (cross marks are 10% melt removal steps), starting from a mantle-derived basaltic melt (“B”) – in these models, “A” is mafic restite contaminant. Arrow describes the composition of a partial melt forming at f=0.95 of the r=0.9 curve. b) McBride data only, with AFC trends starting from an enriched melt “M”, formed as a 30:70 mixture of components “A” and “B”. See text for discussion, composition of end-member components are given in Electronic Annexe EA-1.

Figure 5: Graph of $\delta^{30}Si$ versus a) Mg# and b) Eu/Eu* for the Chudleigh and McBride xenoliths (symbols and error bars as for Figure 1). Trend lines in both plots are for the Chudleigh data only.

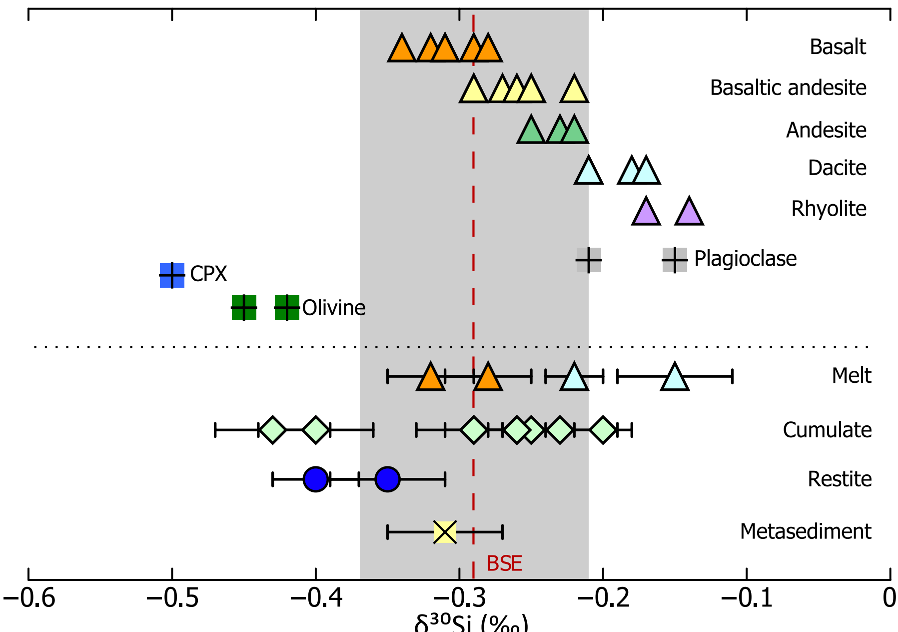

Basalt
Basaltic andesite
Andesite
Dacite
Rhyolite
Plagioclase
CPX
Olivine
Melt
Cumulate
Restite
Metasediment
BSE
−0.6
−0.5
−0.4
−0.3
−0.2
−0.1
0
δ³⁰Si (‰)

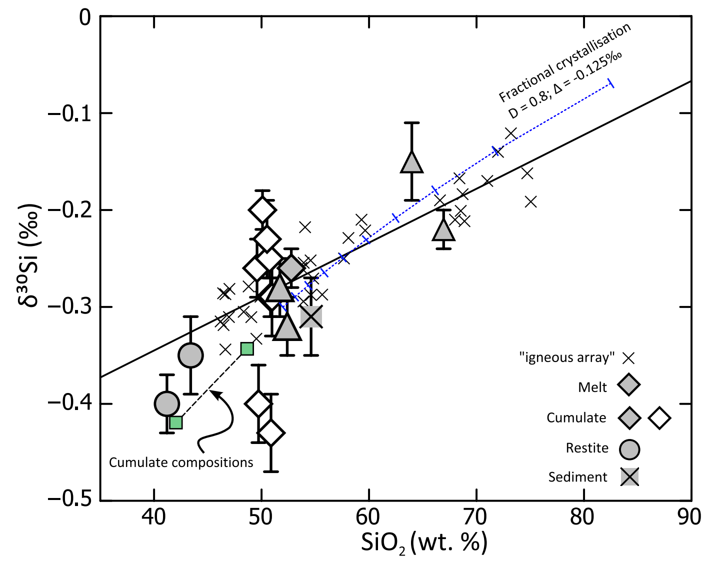

Fractional crystallisation
D = 0.8; Δ = -0.125‰
δ30Si (‰)
SiO2 (wt. %)
"igneous array"
Melt
Cumulate
Restite
Sediment
Cumulate compositions
0
−0.1
−0.2
−0.3
−0.4
−0.5
40
50
60
70
80
90

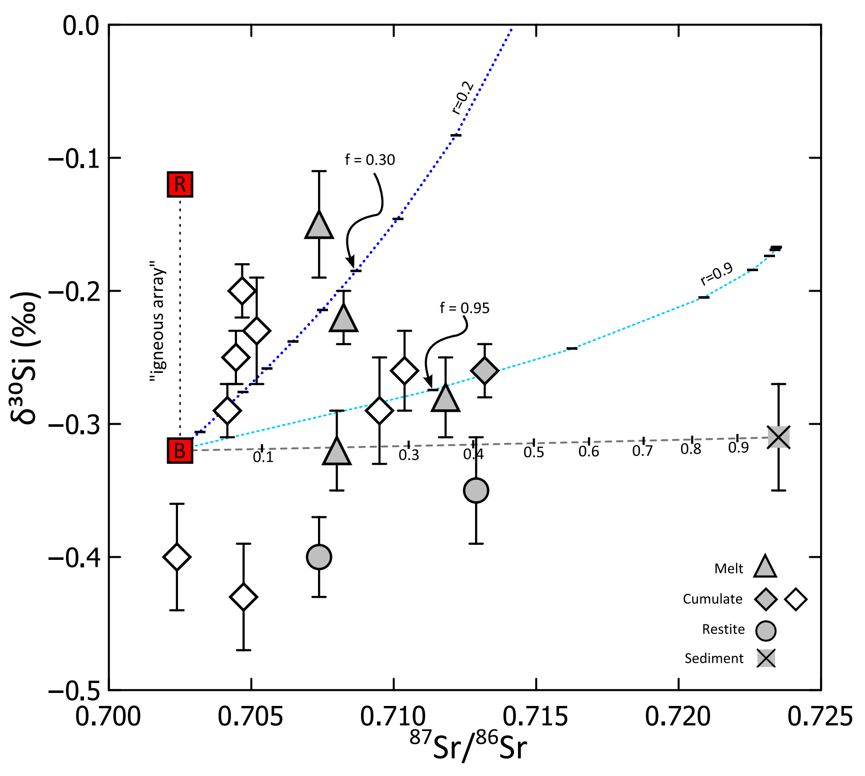

0.0
−0.1
−0.2
−0.3
−0.4
−0.5
0.700
0.705
0.710
0.715
0.720
0.725
$\delta^{30}Si$ (‰)
$^{87}Sr/^{86}Sr$
R
B
"igneous array"
f = 0.30
f = 0.95
r=0.2
r=0.9
0.1
0.3
0.4
0.5
0.6
0.7
0.8
0.9
Melt
Cumulate
Restite
Sediment

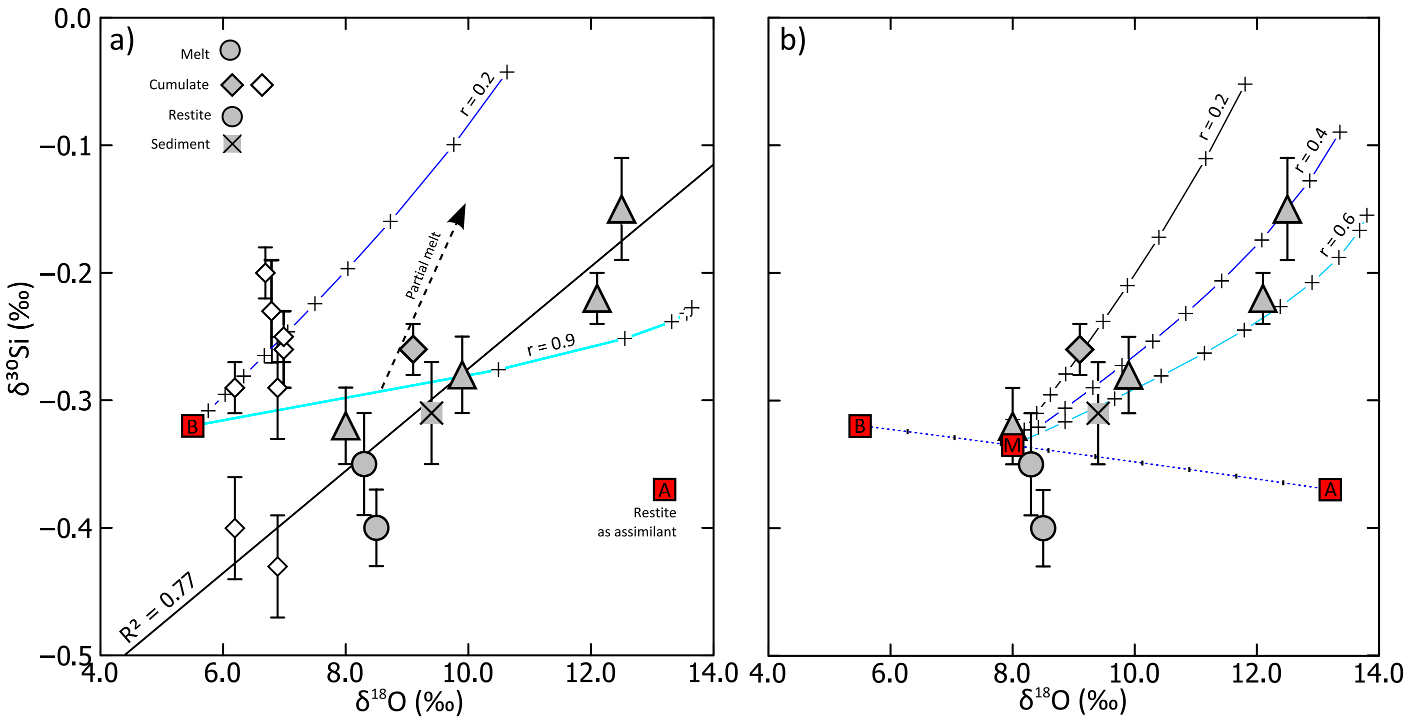

a)
b)
Melt
Cumulate
Restite
Sediment
r = 0.2
r = 0.9
r = 0.4
r = 0.6
Partial melt
R^2 = 0.77
A
B
M
Restite
as assimilant
δ^{30}Si (‰)
δ^{18}O (‰)
0.0
−0.1
−0.2
−0.3
−0.4
−0.5
4.0
6.0
8.0
10.0
12.0
14.0

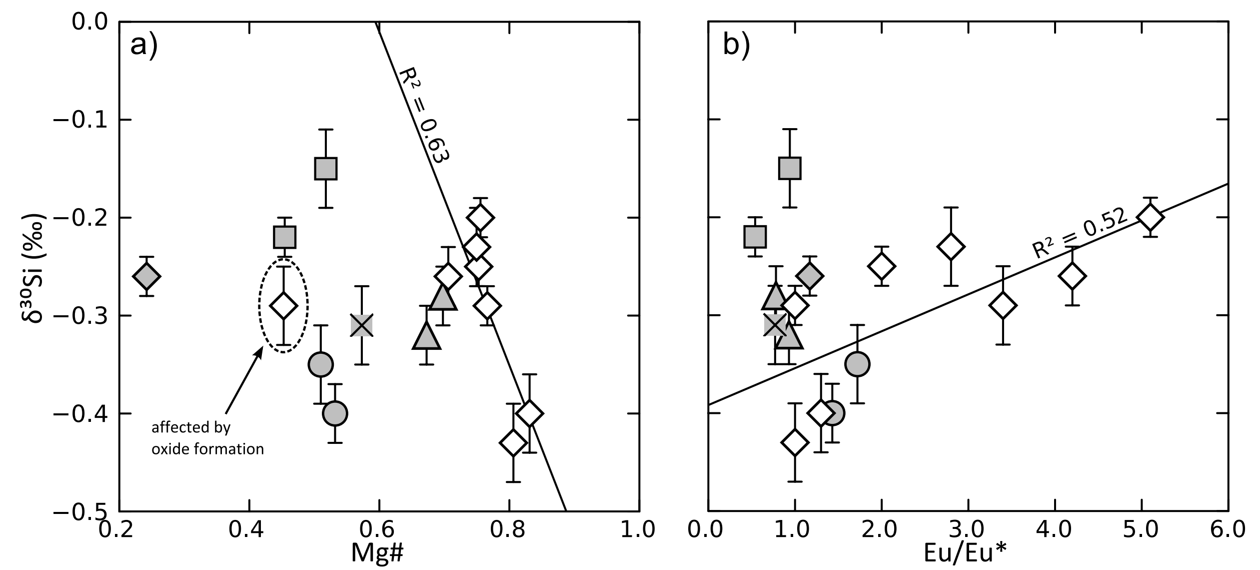

a)
b)
R² = 0.63
R² = 0.52
affected by
oxide formation
δ³⁰Si (‰)
Mg#
Eu/Eu*
0.0
−0.1
−0.2
−0.3
−0.4
−0.5
0.2
0.4
0.6
0.8
1.0
0.0
1.0
2.0
3.0
4.0
5.0
6.0

Table 1. Silicon isotope data for external standards and granulite facies xenoliths

Sample	ID	Description	SiO_2 (wt.%)	$\delta^{30}Si$ (‰)	2s.d.	95%s.e.	$\delta^{29}Si$ (‰)	2s.d.	95%s.e.	*n*	$\delta^{30}Si(m)$ (‰)	off. (%)
BHVO-2	1			-0.31	0.12	0.04	-0.15	0.08	0.03	11		
	2			-0.29	0.07	0.02	-0.13	0.06	0.02	11		
	3			-0.31	0.05	0.02	-0.15	0.05	0.02	11		
	4			-0.26	0.12	0.04	-0.13	0.09	0.03	11		
	Mean/external reproducibility		49.9	-0.29	0.05		-0.14	0.02		4		
Diatomite	1			1.22	0.11	0.04	0.61	0.08	0.03	11		
	2			1.25	0.11	0.04	0.66	0.12	0.04	11		
	3			1.20	0.10	0.03	0.60	0.06	0.02	11		
	4			1.28	0.12	0.04	0.65	0.07	0.02	11		
	Mean/external reproducibility		100.0	1.24	0.07		0.63	0.06		4		
McBride	83-157	Metasediment	54.6	-0.31	0.13	0.04	-0.15	0.11	0.04	11		
	83-159	Mafic restite	43.4	-0.35	0.12	0.04	-0.17	0.08	0.03	10		
	83-160	Felsic melt	64.0	-0.15	0.13	0.04	-0.07	0.07	0.02	11		
	83-162	Felsic melt	66.9	-0.22	0.06	0.02	-0.14	0.06	0.02	9		
	85-100	Mafic melt	51.7	-0.28	0.09	0.03	-0.13	0.08	0.03	11		
	85-107	Mafic cumulate	52.8	-0.26	0.08	0.03	-0.14	0.08	0.03	11		
	85-114	Mafic restite	41.2	-0.40	0.11	0.04	-0.22	0.04	0.01	11		
	85-120	Mafic melt	52.4	-0.32	0.09	0.03	-0.14	0.05	0.02	11		
Chudleigh	83-107	Plag-rich	49.6	-0.26	0.10	0.03	-0.11	0.05	0.02	11	-0.25	5
	83-110	Pyroxene-rich	50.8	-0.29	0.09	0.03	-0.13	0.07	0.02	11	-0.39	33
	83-112(WR)	Plag-rich	51.0	-0.29	0.11	0.05	-0.13	0.09	0.04	8	-0.24	17
	83-115(WR)	Pyroxene-rich	50.9	-0.43	0.12	0.04	-0.21	0.09	0.03	11	-0.39	9

83-125	Plag-rich	50.7	-0.25	0.06	0.02	-0.12	0.09	0.03	11	-0.28	11
83-127(WR)	Plag-rich	50.1	-0.20	0.08	0.03	-0.11	0.08	0.03	11	-0.26	32
83-131	Plag-rich	50.5	-0.23	0.14	0.05	-0.11	0.09	0.03	11	-0.26	15
BC(WR)	Transitional	49.7	-0.40	0.13	0.04	-0.21	0.13	0.04	11	-0.28	30

Silicon isotope data for external standards and whole-rock xenoliths from McBride and Chudleigh volcanic provinces, Australia. Errors are given as 2 s.d. (2 × standard deviation) and 95% s.e. (95% s.e. = t × s.d./(n)1/2, where t = inverse survival function of the Student's t-test at the 95% significance level and n-1degrees of freedom). Silica contents are taken from Rudnick et al. (1986) and Rudnick and Taylor (1987). The δ^{30}Si(m) values are the predicted Si isotopic compositions of the Chudleigh xenoliths, based on their CIPW normative mineralogy and mineral δ^{30}Si analyses taken from Savage et al. (2011). Also shown are the percentage offsets of the model values from their actual isotopic compositions.

Table 2. Silicon isotopic composition of the deep continental crust

	Mafic	Felsic	Int.	Sed.	δ^{30}Si (‰)	2s.d.
	Proportions (%)					
Lower continental crust						
Simple average[a]					-0.29	0.15
Weighted average[b]					-0.28	0.10
Lithological averages[c]						
Archaean	65	15	15	5	-0.28	0.10
Post-Archaean	70	10	10	10	-0.29	0.11
Extensional regions	40	25	25	10	-0.26	0.13
Shield/platform	90	0	0	10	-0.30	0.10
Middle continental crust						
Weighted average[b]					-0.23	0.15
Lithological average[c]					-0.25	0.15

Estimates of the Si isotopic composition of the lower and middle continental crust, calculated via various methods:

[a]simple arithmetic mean.

[b]weighted mean, using the ratio of a sample's SiO_2 content against the average SiO_2 content of the lower or middle crust (53.4 wt.% and 63.5 wt.%; Rudnick and Gao, 2003) and as the weighting parameter.

[c]calculated by first assigning δ^{30}Si values to crustal lithologies, based on the xenolith data, then combining these values using the range of lithological proportions as inferred by Rudnick and Fountain (1995) – see text for details. A range of isotopic compositions for various crustal composites are given.